Chapter 3
Coastal Geomorphology and Tsunami Disaster by the 2011 off the Pacific Coast of Tohoku Earthquake

Tomoya Abe and Kazuaki Hori

Abstract This study investigated the tsunami deposits accumulated at the Pacific coast of Tohoku district by the tsunami associated with the 2011 off the Pacific coast of Tohoku Earthquake. Influence of coastal landforms on the tsunami deposits and run-up heights was also discussed. Pleistocene terraces, rias, strand plain, and valley plain surrounded by terraces or hills occur generally along the coast from north to south. Tsunami deposits up to several tens of centimeters in thickness accumulated broadly in strand plain and valley plain. Although thick tsunami deposits also formed at small bay-head deltas in rias, tsunami deposits were not clear and erosional landforms caused by tsunami backwash were common in a very small, steep valley plain along the ria coasts. Sandy deposits show landward-thinning trend at wide strand plain and valley plain. However, the similar trend was not clear at narrow strand plain. The difference is probably related to decrease in sediment transport capacity of the tsunami and sediment supply. Sediment distribution and run-up height are strongly influenced by onshore topography. In high-lying topography, run-up height may relate to onshore slope and shape of lowland. On the other hand, run-up height is possibly controlled mainly by the characteristics of incident wave (wave period and height) in low-lying topography. Further detailed investigation about submarine topography is also required in the near feature.

T. Abe (✉)
Marine Geology Research Group, Institute of Geology and Geoinformation, Geological Survey of Japan, Tsukuba Central 7, 1-1-1 Higashi, Tsukuba, Ibaraki 305-8567, Japan
e-mail: tomoya-abe@aist.go.jp

K. Hori
Department of Geography, Graduate School of Environmental Studies, Nagoya University, D2-2 Furocho, Chikusa-ku, Nagoya Aichi 464-8601, Japan

3.1 Introduction

The 2011 off the Pacific coast of Tohoku Earthquake (*Mw* 9.0) occurred on March 11, 2011. The earthquake triggered huge tsunami (hereinafter called the 2011 Tohoku-oki tsunami), and the tsunami inundated and damaged to the wide range of the coastal areas facing the Pacific Ocean in the northeast Japan. In particular, coastal area in Iwate, Miyagi, and Fukushima prefectures was mostly damaged by huge tsunami.

Tsunami causes huge sediment transport near coastal area. Sediment formed by tsunami is called "tsunami deposit". Researches of tsunami deposits can provide useful information of past tsunamis to aid in the future assessment of the tsunami hazard (Goff et al. 2012). Tsunami deposits on coastal lowlands are useful for estimating recurrence intervals and magnitudes of ancient tsunami events. It enables us to expand our knowledge on the history of past tsunamis older than thousands of years ago. For example, maximum inland extent of tsunami deposits is assumed to represent a minimum of inundation distance (Jaffe and Gelfenbaum 2002; Koshimura et al. 2002; Nanayama et al. 2003).

Maximum landward extent of the sandy tsunami deposits can be regarded as the minimum inundation limit. Before the 2011 Tohoku-oki tsunami, recent post-tsunami field surveys along low-lying coastlines showed that sandy tsunami deposits commonly extend to approximately over 90 % of the actual inundation limit (MacInnes et al. 2009). On the other hand, after the 2011 Tohoku-oki tsunami, some researches of the 2011 tsunami pointed out that there was the significant gap (0.6–2.0 km) between the inundation limit and the maximum landward extent of the sandy tsunami deposit where the inundation distance was more than 2.5–3.0 km (Goto et al. 2011; Abe et al. 2012; Shishikura et al. 2012).

Case studies of recent tsunami impacts have proven to be extremely useful in understanding the geological processes involved in inundation and return flow, and refining the criteria to identify paleo-tsunami deposits in the geological record (Richmond et al. 2012). Many studies were conducted after recent tsunamis including 2004 Indian Ocean tsunami and the 2011 Tohoku-oki tsunami. In general, tsunami deposits thin and fine landward, although local microscopic topographic features give strong effects to the distribution trend of the deposits. Post-tsunami field surveys after the 2011 Tohoku-oki event revealed that the thickness and grain size varied significantly because of the small-scale undulations (Nakamura et al. 2012), redistribution of the vented sediments from liquefaction (Goto et al. 2012), and scouring at the lee side of engineering structures (Takashimizu et al. 2012).

Onshore tsunami behavior, mainly characterized by run-up height, inundation height, inundation distance, velocity, and direction, widely varied depending on coastal geomorphology. Several types of coastal geomorphology are distributed along the coasts of Iwate, Miyagi, and Fukushima prefectures. For example, central to southern parts of Iwate Prefecture to northern part of Miyagi Prefecture are well known to the development of rias, whereas strand plains are distributed at the southern parts of Miyagi Prefecture. Geomorphological approaches to deposition,

erosion, and flow characteristics of the tsunami were applied to ria coast (e.g., Komatsu et al. 2014; Hayakawa et al. 2015). However, difference of distribution pattern of the tsunami deposit and tsunami height among these coasts was poorly understood.

In this paper, we reported the characteristics of the tsunami deposits formed by the 2011 Tohoku-oki tsunami based on the field survey. We also discussed the influence of the onshore landform on the tsunami deposits and run-up heights.

3.2   Regional Setting

The study area belongs to non-volcanic outer arc in the northeast Japan. Most of the study area except for the northern end and central part is located at the east side of the Kitakami and Abukuma mountains characterized by gentle plateau-like topography. The Kitakami Mountain is underlain largely by Palaeozoic and Mesozoic sedimentary rocks and the Lower Cretaceous granitic rocks and has the elevation of 600–1300 m. The Abukuma Mountain consists mainly of the Cretaceous granitic rocks, metamorphic rocks, and Palaeozoic and Mesozoic sedimentary rocks. The mountain is bordered on the northeast by the Futaba Fault. Neogene sedimentary rocks are common along the coast on the east side of the mountain.

The coast faces the Pacific Ocean. Tidal range along the coast is around 1 m (National Astronomical Observatory of Japan 2013). Yearly average significant wave height ranges from 0.6 to 1.2 m at stations along the coast in 2013 (Kawaguchi et al. 2015). Maximum significant wave heights, 4.0–7.5 m, were associated with tropical cyclones and low pressures.

Coastal landforms can be roughly divided into four areas from north to south based on their characteristics. These areas are called conveniently as Kamikita Plain, Sanriku Coast, Sendai Plain, and Iwaki Coast (Fig. 3.1). Geomorphic studies about these coastal landforms were summarized by Koike et al. (2005).

Marine terraces occur widely at the Kamikita Plain. The terraces are dissected by rivers flowing into the Pacific Ocean and fluvial terraces formed by these rivers. The distribution of the marine and fluvial terraces combined with tephrostratigraphic studies suggests that the plain has uplifted since at least ca. 430–470 ka (Miyauchi 1987). Furthermore, the uplift rate along the coast is estimated to be 0.1–0.2 mm/year during the last 120 ka (Miyauchi 1987).

Coastal cliffs and smoothly shaped coastlines are common along the northern part of the Sanriku Coast. Middle to Late Pleistocene marine terraces also develop well at the coast like the Kamikita Plain (Yonekura 1966). Elevation of the highest terrace called "Mizunashi Surface" ranges from 80 to 280 m above sea level and is estimated to be built at marine isotope stage (MIS) 19, ca. 760 ka (Miyauchi 2001).

In contrast, indented coastlines characterize the middle and southern parts of the Sanriku Coast. Many rias with long and narrow inlets are distributed at river mouths originated from the Kitakami Mountain. Water depth at each bay entrance is usually
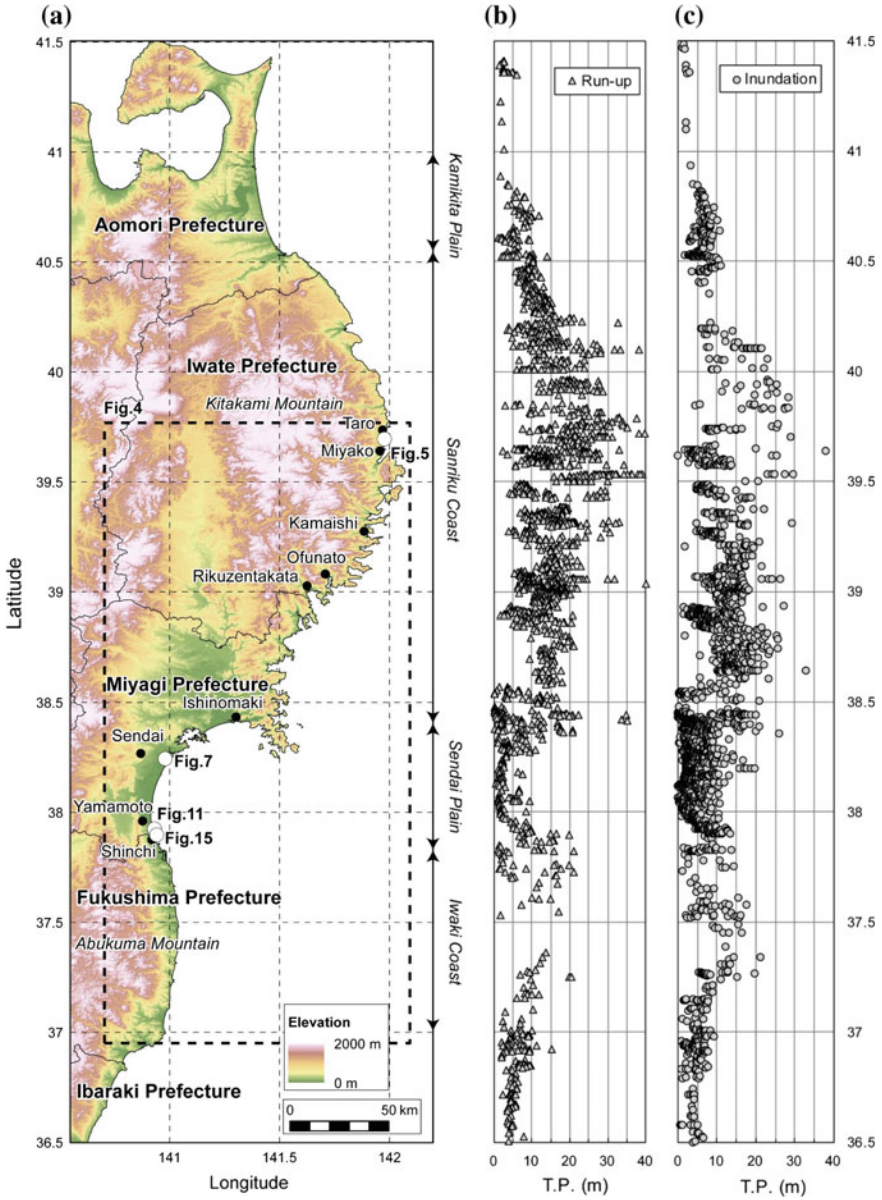
Fig. 3.1 **a** Elevation map of study area using 10 m mesh digital elevation model (DEM) provided by the Geospatial Information Authority of Japan (GSI), location of survey sites and main cities, **b** run-up height above Tokyo Peil (TP), **c** inundation height above TP provided by the 2011 Tohoku Earthquake Tsunami Joint Survey Group (TETJSG) (2011)

around 100 m. Thus, the bay reduces water depth rapidly landward. The original shape of the rias was probably formed around the latest Neogne to the earliest Pleistocene, ∼2 Ma due to the submergence of valleys cutting into the Kitakami Mountain (Yoshikawa 1964, 1997; Miura 1968), though no absolute ages have been obtained. Marine terraces occur fragmentally along the valley wall of the rias and the present coast (Yoshikawa 1964; Miura 1966, 1968). For example, the formation age of the highest terrace distributed around Kesennuma may be corre-lated with MIS 11, 400 ka (Yagi and Suzuki 2001), though tephrochronology could not have been available for the terrace. The presence of the terraces implies that the middle and southern parts of the Sanriku Coast have uplifted. The rias have been generally less sedimentary filling. As the rivers through the Kitakami Mountain are small in length and cut the Palaeozoic to Mesozoic hard sedimentary rocks, fluvial sediment supply to the rias has been small. However, relatively minor coastal lowlands (e.g., bay-head delta) can be found at the head of some rias. For example, thick sedimentary sequence (i.e., incised-valley fill) accumulated during deglaciated sea-level rise and highstand following low sea-level phase at the Last Glacial Maximum was reported from the Rikuzentakata coastal plain built by the Kesen River (Chida et al. 1984). Several cities such as Miyako, Kamaishi, Ofunato, Rikuzentakata, and Kesennuma with estimated population of ca. 19,000–65,000 are distributed at these lowlands.

Sendai Plain extends between the southern end of Kitakami and the northern end of Abukuma mountains. There are two widespread strand plains under wave-dominated condition. The northeastern part usually called as Ishinomaki coastal plain with 20 km in length and 9 km in maximum width has been formed at the lower reach of the Kitakami, Eai, and Naruse rivers (Matsumoto 1981b; Ito 1999). The southwestern part called as Sendai coastal plain with 50 km in length and 10–15 km in maximum width has been built at the lower reach of the Nanakita, Natori, and Abukuma rivers (Matsumoto 1981a). Elevation of both plains is gen-erally less than 5 m. Several beach ridges almost parallel to the present shoreline develop well at both plains. They have been formed during the sea-level highstand since the mid-Holocene (Matsumoto 1984). Back marsh underlain by organic-rich mud occurs widely landward and between the beach ridges. Relative elevation between back marsh and beach ridge is approximately 0.5–1.5 m. Natural levees and the former river channels are also developed along the rivers.

Late Pleistocene to Holocene sediment thickness reaches approximately 60 m under the present coast (Matsumoto 1981b). Incised valleys were formed in response to sea-level lowering and were filled by fluvial and marine deposits during the subsequent sea-level change. In particular, the Holocene succession, <30 m thick, overlies latest Pleistocene to Early Holocene non-marine deposits in the Sendai coastal plain (Tamura and Masuda 2005). It is composed of ravinement, inner shelf, and shoreface to coastal plain deposits (Tamura and Masuda 2005).

Valley plain, fluvial and marine terraces, and hills occur repeatedly from north to south along the smoothly shaped Iwaki Coast. Rivers from the Abukuma Mountain into the Pacific Ocean and each landform generally extend east–west direction. In particular, the terraces become to cover a larger area toward south. Elevation of the

terraces formed at MIS 5e suggest that uplift rate along the coast is 0.2 mm/year in the north and 0.5 mm/year in the south (Suzuki 1989). Shore erosion has retreated coastal cliffs composed of Neogene soft sedimentary rocks rapidly and has resulted in the formation of widespread abrasion platform. Valley plains are surrounded by the terraces and hills to the north and south. Lagoons are often found along the coast where sedimentary filling by the rivers has been not enough. Land reclamation has changed some of these lagoons into paddy field.

Sea-level change during the Holocene was estimated from Rikuzentakata coastal plain and Sendai coastal plain based on age–depth plots of peat, wood piece, and molluscan shells (Chida et al. 1984; Matsumoto 1981a). According to these studies, sea level has reached close to the present level around 5 ka. Sea level has been almost stabilized since the mid-Holocene, though small fluctuations, $\sim$1–2 m, have been estimated.

3.3 Method

We conducted field survey in four areas having different topographic features (Fig. 3.2). Landform types are very small, steep gradient valley plain along the north end of ria coasts (Matsutsuki, Iwate Prefecture), wide strand plain (Sendai, Miyagi Prefecture), narrow strand plain (Yamamoto, Miyagi Prefecture), and valley plain surrounded by hills (Shinchi, Fukushima Prefecture). We observed tsunami deposit formed by the 2011 tsunami in Sendai, Yamamoto, and Shinchi areas. On the other hand, geological survey of the tsunami deposit was not conducted in Matsutsuki area, because erosional features were dominant and we hardly found the tsunami deposit.

Three shore-normal transects were established to determine the inundation limit of the Tohoku-oki tsunami in Sendai, Yamamoto, and Shinchi areas (Fig. 3.1). The inundation limit, run-up heights, and inundation heights and depths (Fig. 3.3) along each transect were identified based on the tsunami-deposited debris, watermarks, and eyewitness accounts of local people during our field survey from April to June, 2011. The topography (elevation) from the coastline to the inundation limit was measured along each transect using RTK GPS instruments (Promark 3; Ashtech). We adopted the inundation heights and run-up heights measured by the Tohoku Earthquake Tsunami Joint Survey Group (TETJSG) (2011) near the transects. Trench surveys of the tsunami deposit were conducted at 86 sites spaced about 30–100 m apart on average along each transect. Thickness of the tsunami deposit was documented at each site, and erosional features of the tsunami were observed at each area.

We use run-up height database of TETJSG (2011) in order to examine relationship between average onshore slope from the shoreline to inundation limit and run-up height at inundation limit in various types of coastal landform from the middle part of Sanriku to Iwaki coasts. TETJSG database totally includes run-up data at 1962 points in the coasts shown in Fig. 3.1 (N41.5°–N36.5°). We selected
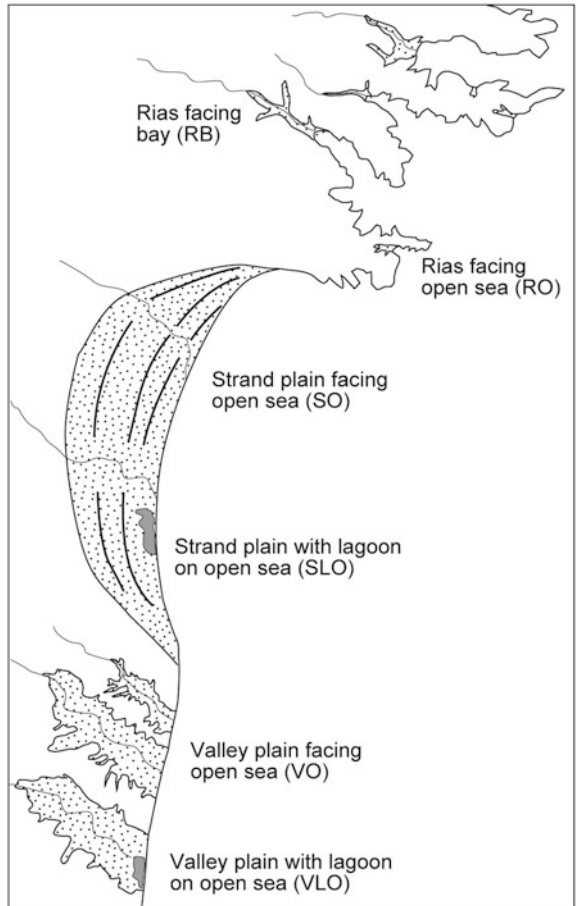
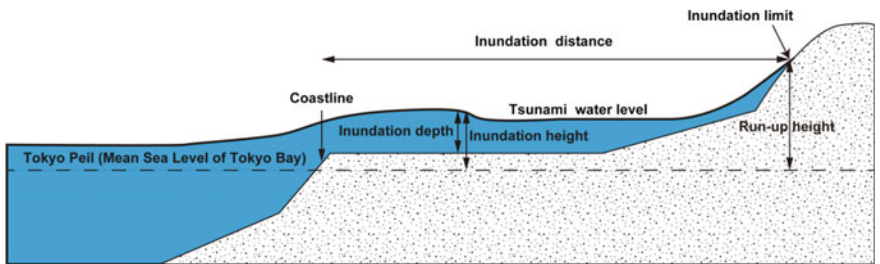**Fig. 3.2** Topographic types in study area

Fig. 3.3 Definition of inundation distance, inundation height, inundation depth, inundation limit, and run-up height in this study

the data based on some geomorphological criteria. Firstly, we removed the data obtained at terrace cliff, because onshore slope may not be associated with run-up height at terrace cliff. Secondly, we excluded the data within the rivers and channels on the ground that rivers have highly potentially extend inundation distance and height irrespective of onshore slope. We also excluded the data where high seawall or gate for tsunami protection, for example, Taro-cho, Fudai-mura, and Kamaishi-city in Iwate Prefecture, was constructed. These structures may decrease the run-up height. Finally, we chose 117 points (Fig. 3.4) from various types of coastal landform under the standards described above. Landforms at these points are classified into six types. Here, we conveniently call them as rias facing open sea (RO), rias facing bay (RB), valley plain facing open sea (VO), valley plain with lagoon on open sea (VLO), strand plain on open sea (SO), and strand plain with lagoon on open sea (SLO) (Fig. 3.2).

3.4 Results

3.4.1 Small, Steep Valley Plain Along the Ria Coasts

This valley is located at Matsutsuki between Taro-cho and Miyako city, Iwate Prefecture (Fig. 3.1), north end of ria coasts. The valley extends east–west to southeast–northwest direction (Fig. 3.5a) and is surrounded by hills with over 50 m height (Fig. 3.5b). The width of the main valley is only 100–200 m. The coastline faces directly the open ocean and is covered with sandy and gravelly sediments.

The run-up height is 27–30 m above from the Tokyo Peil (TP) near the shoreline. Inundation area mostly covered main valley and branch valleys (Fig. 3.5a). Tsunami inundated up to 1.20 km inland from the shoreline and 29.3 m above TP (TETJSG 2011). Run-up flow stopped due to steep slope (Fig. 3.6a). The gradient between the inundation limit and the shoreline was 24.10 ‰ on average.

Erosional features were dominant in this valley. Trees and grasses at the lower part (less than about 30 m above TP) of the valley wall were lost by the tsunami (Fig. 3.6a). Backwash flow formed narrow channel with 100 m long, 5 m width, and 1–2 m depth (Fig. 3.6b) and mostly discharged paddy soil distributed before the tsunami into the sea. Since it is difficult to observe the deposition by the tsunami, we did not conduct geological survey of the tsunami deposit.

3.4.2 Wide Strand Plain

We set the 4.02-km-long transect from the shoreline to inundation limit in the northern part of the Sendai coastal plain located at Sendai City in middle part of Miyagi Prefecture (Fig. 3.1). The transect is almost parallel to the present Nanakita
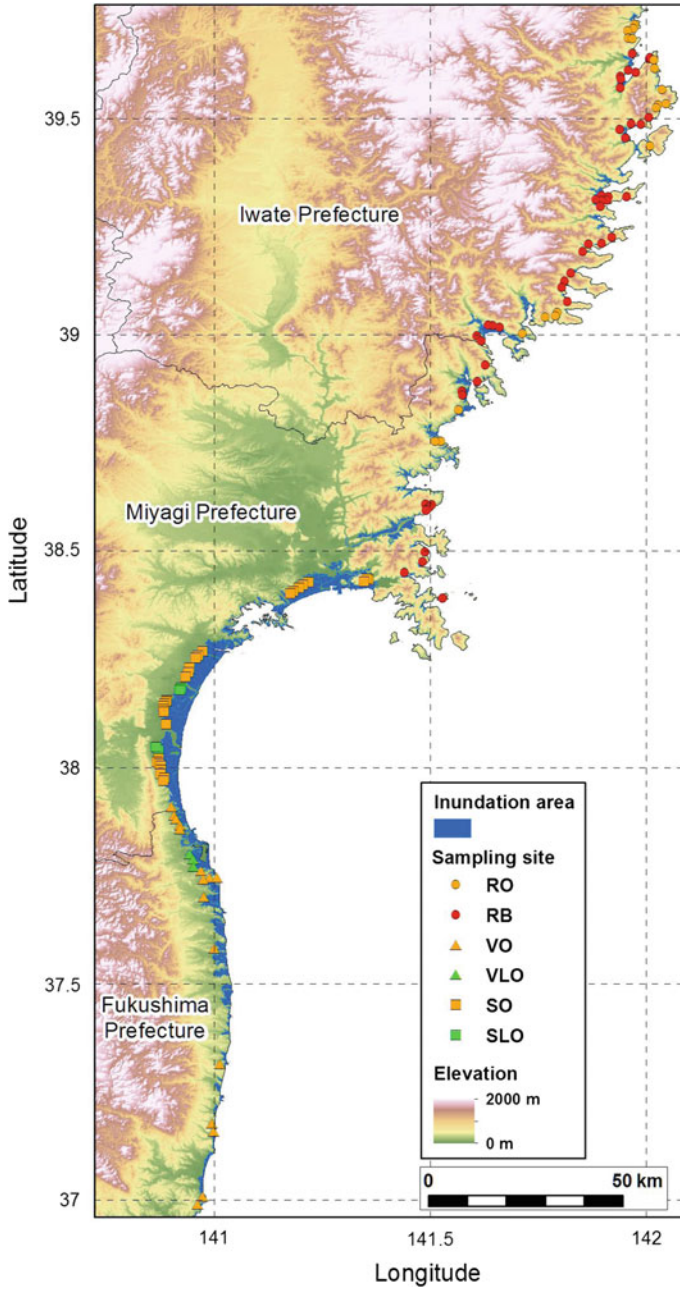
Fig. 3.4 Elevation map using 10 m mesh DEM of study area, inundation area provided by Ministry of Land, Infrastructure, Transport and Tourism, and location of analyzed run-up height data provided by TETJSG (2011)
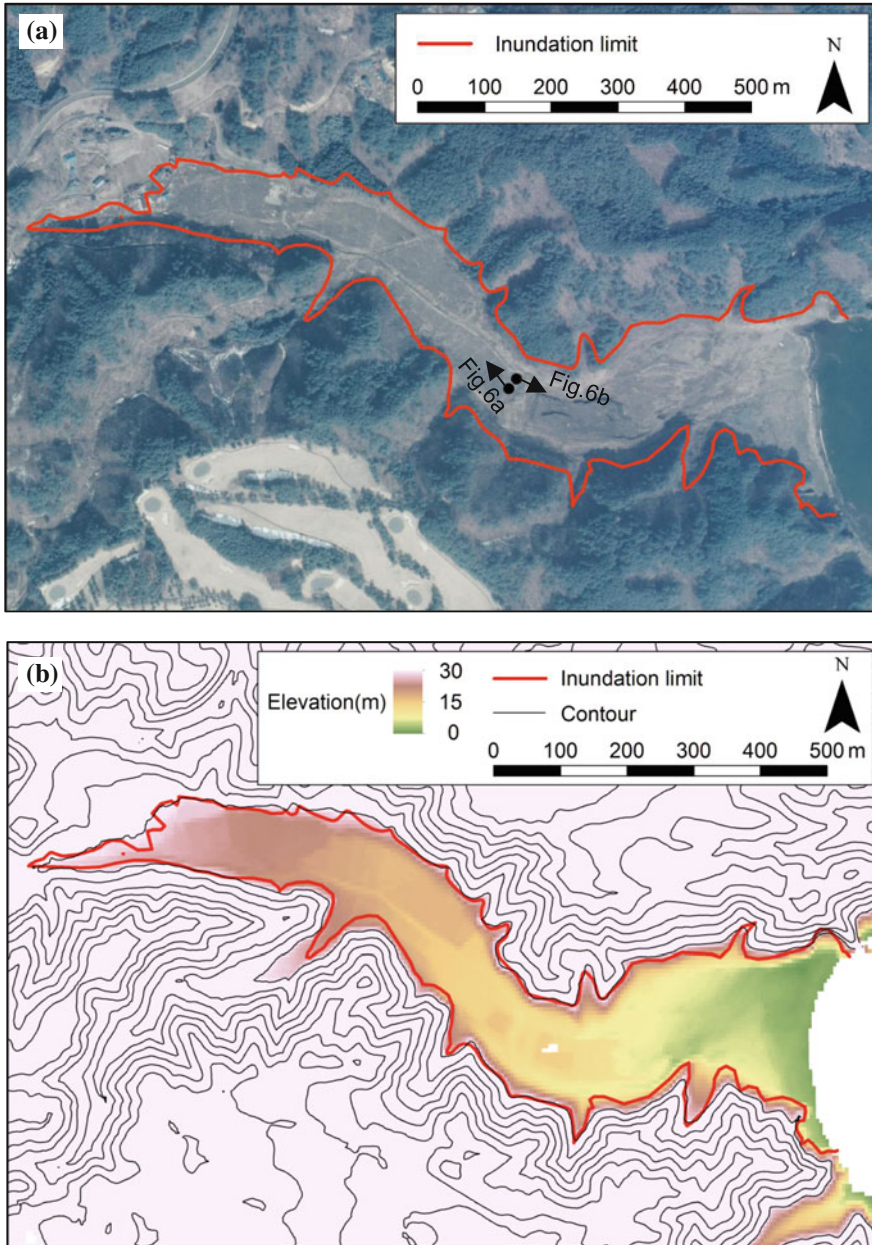
Fig. 3.5 **a** Aerial photograph (March, 2011) provided by GSI, inundation area, shooting locations and direction of photographs in Fig. 3.6, **b** elevation map using 5 m mesh DEM provided by GSI, 10 m interval contour line (except for less than 20 m above T.P.), and inundation area in rias at Matsutsuki. The location is shown in Fig. 3.1
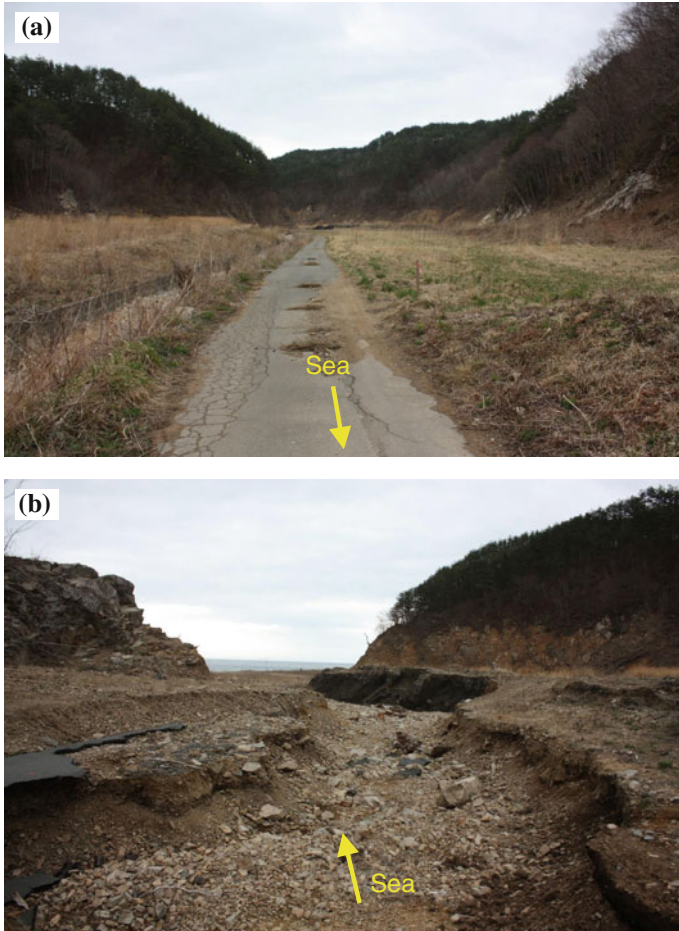
Fig. 3.6 Photographs of (**a**) steep gradient topography and (**b**) channel formed by the tsunami backwash in rias at Matsutsuki. Shooting locations and direction of photographs are shown in Fig. 3.5a

River flowing along the northern side of the transect. The survey area mainly covered the following topographies and structures landward: (a) 0.13-km-wide sandy beach, (b) 6.2-m-high onshore seawall, (c) 2–3-m-high sand dune, (d) 0.62-km-wide coastal forest planted pine tree behind the beach, and (e) low-lying rice paddy field that extends from 0.75 to 3.93 km from the coastline (Fig. 3.7a). Local subsidence of 0.2 m occurred by the 2011 earthquake according to real-time observation of the GSI electronic reference point near this transect.

The tsunami inundated up to 4.02 km inland from the shoreline and 3.1 m above TP at a maximum (TETJSG 2011) (Fig. 3.7b) due to flat topography (Fig. 3.8a). Tsunami eroded sand beach and dune with 2 m depth at a maximum (Fig. 3.8b) and
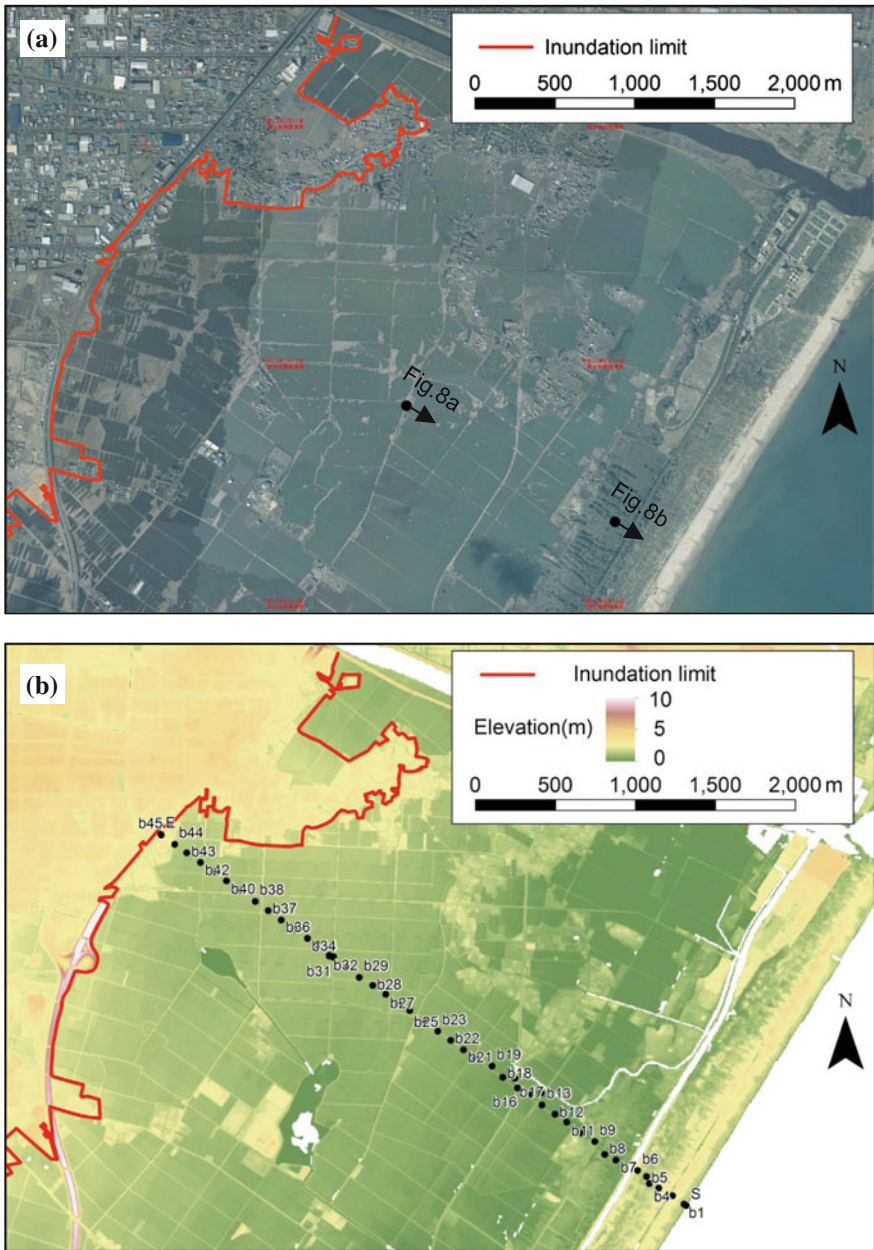
Fig. 3.7 **a** Aerial photograph (March, 2011) provided by GSI, inundation area, shooting location and direction of photograph in Fig. 3.8, **b** elevation map using 5 m mesh DEM, inundation area, and observation sites of the tsunami deposit in wide strand plain at Sendai City. The location is shown in Fig. 3.1

Fig. 3.8 Photographs of (**a**) flat topography and coastal trees transported by the run-up flow and **b** erosion in sand dune in wide strand plain at Sendai City. Shooting locations and direction of photographs are shown in Fig. 3.7a

transported inland huge amount of beach and dune sand, and many pine trees planted on sand dune (Fig. 3.8b) with a long distance (Fig. 3.8a). Additionally, paddy soil landward of the road was eroded with several tens of centimeters depth. Inundation heights were 6.3 m above TP landward of the coastal forest and decreased inland (Fig. 3.9a). Inundation depths were 3 m at 1.6 km from the

shoreline and decreased inland. The average gradient between the inundation limit and the shoreline was 0.77 ‰.

The tsunami deposit was described every 50–100 m at 45 sites (b1-b45) shown in Fig. 3.7b. The tsunami sand layer and mud layer were composed of 0.1–34-cm-thick fine-to-medium sand and 0.1–3-cm-thick silt, respectively (Figs. 3.9b and 3.10). Generally, sand thickness thinned landward, and mud thickness gently became thicker landward. However, the sand and mud thickness fluctuated in associated with local topography. Up to a distance of 0.1 km from the shoreline, tsunami deposit was not observed and erosion was dominant in sand beach. Between 0.1 and 1.2 km from the shoreline, the deposit was composed of 1–34-cm-thick, medium-grained sand layer. Between 1.2 and 3.0 km inland, the
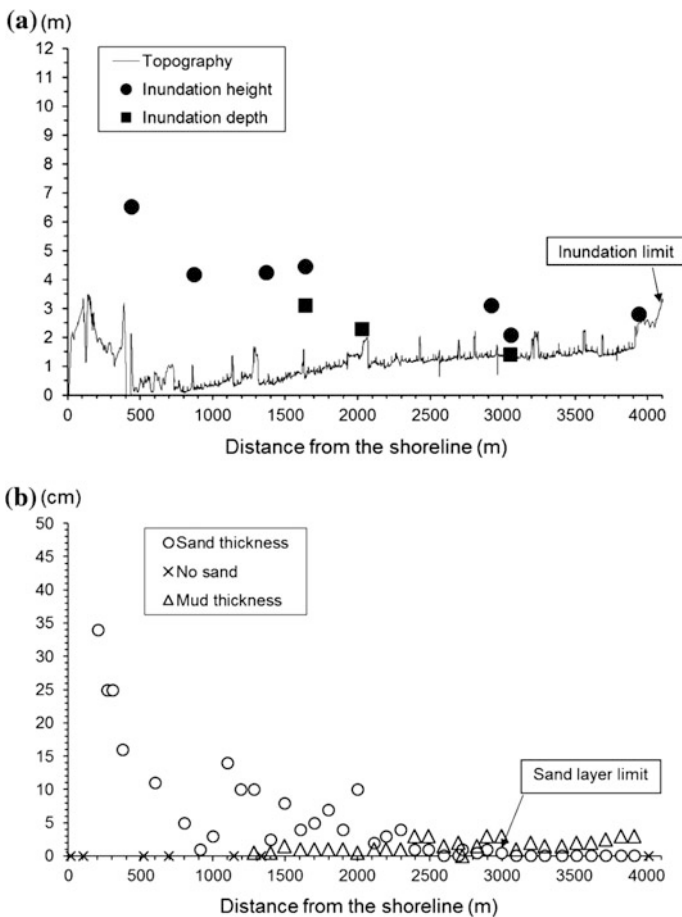

Fig. 3.9 **a** Elevation (m), inundation height (m) above TP, inundation depth (m), and inundation limit, **b** sand thickness (cm) and mud thickness (cm) along the transect in wide strand plain at Sendai City

Fig. 3.10 11-cm-thick sand layer at 0.6 km from the shoreline (site b8 in Fig. 3.7b) in wide strand plain at Sendai City

tsunami deposit was sand-dominated and was composed of 0.5–10-cm-thick fine- to medium-grained sand layer with a mud cap in 0.1–3 cm thickness. Further inland (3.0–4.0 km), the deposit became mud-dominated and was composed of 1–3-cm-thick mud overlying a patchy thin layer of massive fine- to medium-grained sand (0.1–0.3 cm thick).

The tsunami sand layer thicker than 0.5 cm was found up to approximately 3.0 km inland, which corresponds to 74.5 % of the inundation distance. The submillimeter (sub-mm) tsunami sand layer and the mud layer were found up to approximately 3.9 km inland, which is equal to 97.3 % of the inundation distance.

3.4.3   Narrow Strand Plain

We set the 0.60-km-long transect in narrow strand plain located at Yamamoto Town in southern part of Miyagi Prefecture (Fig. 3.1). This plain included in the Sendai coastal plain is located about 40 km south of Sendai City. The survey area covered (a) 0.03-km-wide sandy beach, (b) 6.2-m-high onshore seawall, (c) 2–3-m-high sand dune, (d) 0.14-km-wide coastal forest planted pine trees behind the beach, and (e) low-lying rice paddy field and dry field planted vegetables before the tsunami that extend from 0.17 to 0.60 km from the coastline. Local subsidence of 0.26 m occurred by the 2011 earthquake according to real-time observation of the GSI electronic reference point near this transect.

Tsunami inundated up to 0.60 km inland (Fig. 3.11a). Inundation area was limited by the occurrence of high terraces (over 15 m height) (Figs. 3.11b and 3.12a). Tsunami eroded the sandy beach and dune and formed a small "Tsunami Bay" landward side of the seawall (Fig. 3.12b). Inundation heights were 11.3 m above TP near the beach and slightly decreased landward (Fig. 3.13a) (TETJSG 2011). Run-up flow stopped at terrace cliff.
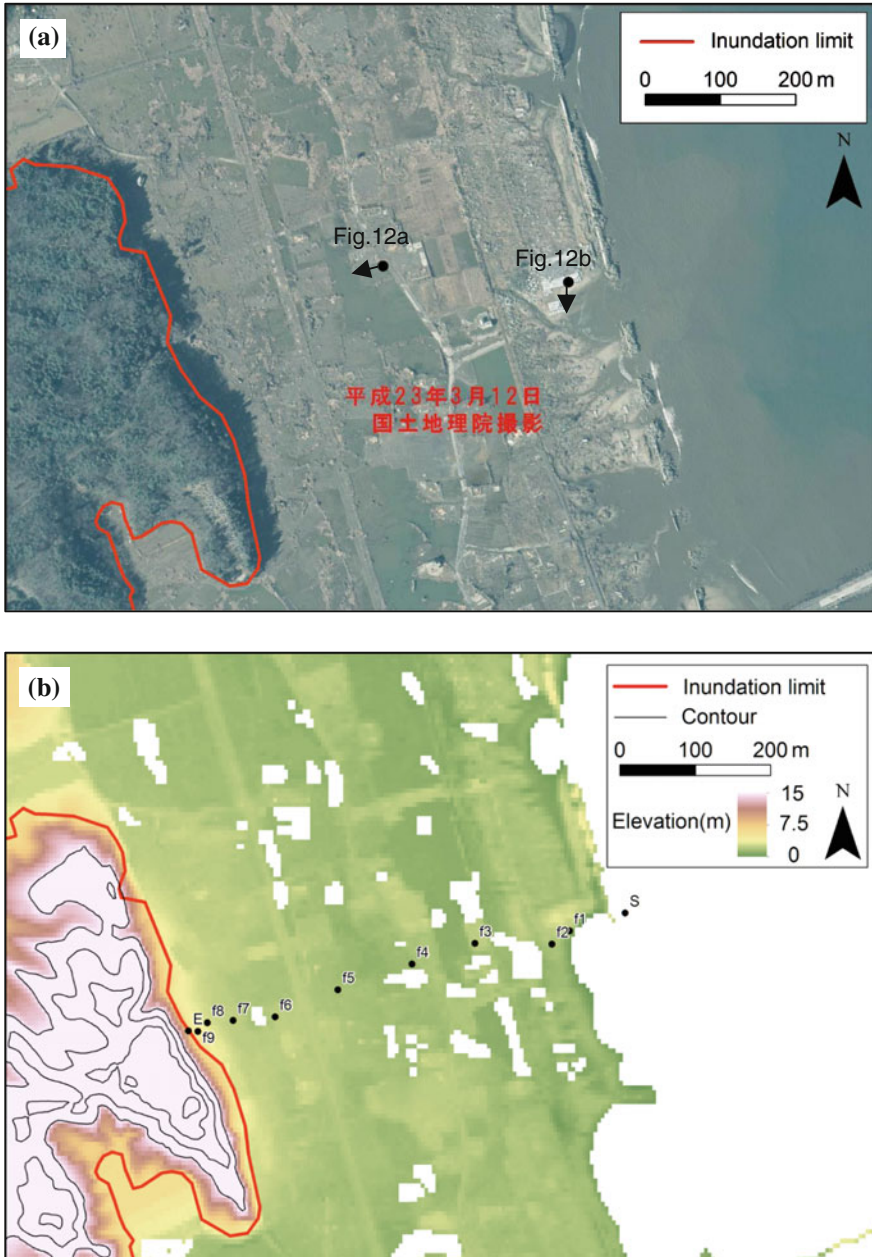
Fig. 3.11 **a** Aerial photograph (March, 2011) provided by GSI, inundation area, shooting location and direction of photograph in Fig. 3.12, **b** elevation map using 5 m mesh DEM, 5 m interval contour line (except for less than 10 m above TP), inundation area, and observation sites of the tsunami deposit in narrow strand plain at Yamamoto Town. The location is shown in Fig. 3.1
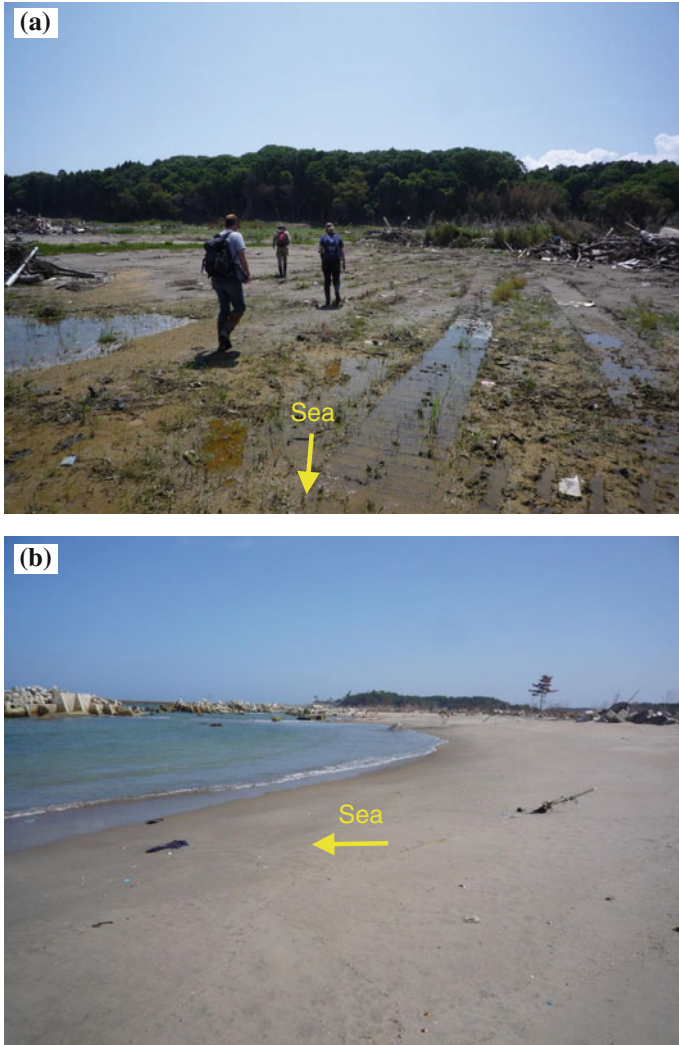
Fig. 3.12 Photographs of **a** lowland and terraces and **b** erosion in sand beach and dune in narrow strand plain at Yamamoto Town. Shooting locations and direction of photographs are shown in Fig. 3.11a

The tsunami deposit was described every 30–100 m at 9 sites (f1–f9) in Fig. 3.10b. Sand layer was composed of 4–12.5-cm-thick fine- to medium-grained sand (Figs. 3.13b and 3.14). Generally, sand thickness did not clearly thin landward. No sand was observed up to a distance of 0.25 km from the coastline, because erosion was dominant. Between 0.25 and 0.59 km inland from the shoreline, the deposit was mainly composed of 4–12.5-cm-thick, fine-to-medium sands overlain by thin mud (0.2–0.5 cm thick). Mud thickness was generally very thin than other areas. At the maximum extent of the tsunami deposits, the sand unit
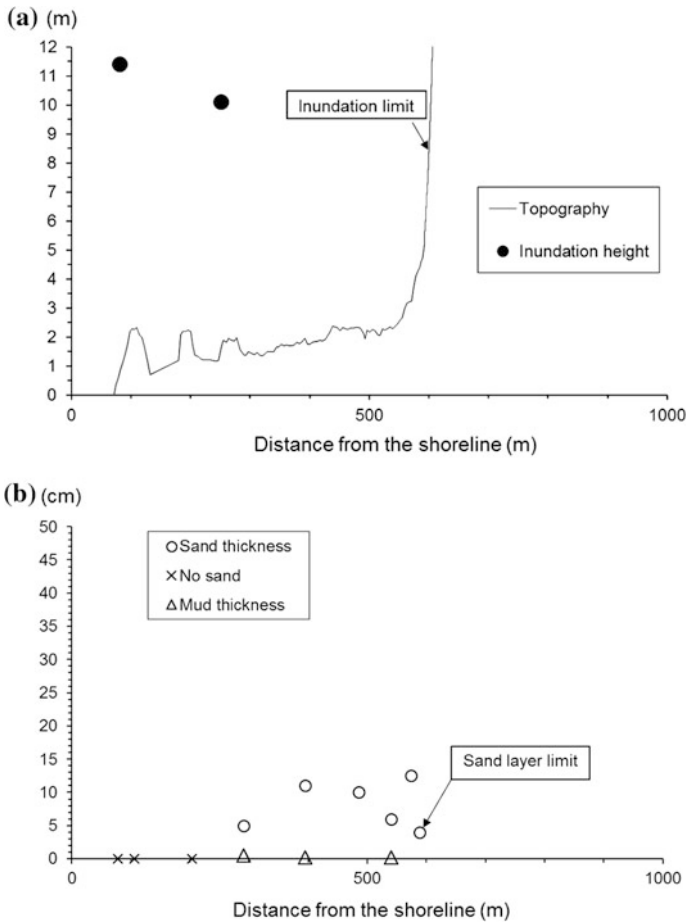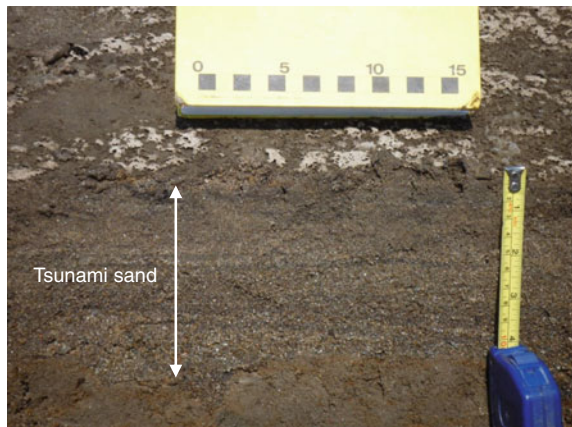
Fig. 3.13 a Elevation, inundation height above TP, and inundation limit, **b** sand and mud thickness in narrow strand plain at Yamamoto Town

Fig. 3.14 10-cm-thick sand layer at 0.4 km from the shoreline (site f8 in Fig. 3.11b) in narrow strand plain at Yamamoto Town

had 4 cm in thickness. Sections of the tsunami deposit with a submillimeter and over 0.5-cm-thick sand layer were found up to approximately 0.59 km inland (98.2 % of the inundation distance).

3.4.4 Valley Plain

We surveyed a valley plain developed at Shinchi Town in northern part of the Fukushima Prefecture (Fig. 3.1). This valley plain is located on a coastal lowland, about 42 km south of Sendai City. The valley extends east–west direction (Fig. 3.15a) and is surrounded by hills with over 15–30 m height (Fig. 3.15b). The survey area covered (a) 0.04-km-wide sandy beach, (b) 6.2-m-high onshore seawall, (c) 3-m-high sand dune, (d) 0.16-km-wide coastal forest planted pine trees behind the beach, and (e) the rice paddy field that extends from 0.23 to 2.23 km from the coastline. The site was subsided locally with 0.31 m by the 2011 earthquake according to real-time observation of the GSI electronic reference point near this transect.

The tsunami inundated up to 2.23 km inland and 6.9 m above TP (Fig. 3.15b). Run-up flow would be forcibly stopped probably due to steep slope (Fig. 3.16a). Tsunami eroded sandy beach and dune and formed "Tsunami Bay" (Fig. 3.16b). Inundation height near the coast was approximately 8.5 m above TP and decreased landward (TETJSG 2011) (Fig. 3.17a). The average gradient between the inundation limit and the shoreline was 3.09 ‰.

The tsunami deposit was surveyed every 30–100 m at 32 sites (m1-m32) in Fig. 3.15b. The tsunami sand layer and mud layer were composed of 0.5–28-cm-thick fine-to-medium sand and 0.1–5.5-cm-thick silt, respectively (Figs. 3.17b and 3.18). Sand thickness generally thinned landward and fluctuated in associated with local duration. Mud thickness gradually became thicker inland. Erosion was dominant up to 0.2 km from the coastline (Fig. 3.17b). Between 0.2 and 0.45 km inland from the shoreline, sandy deposit was dominant and 5–28-cm-thick fine- to very coarse-grained sand layer was formed. Further inland (0.45–2.05 km), the tsunami deposit was sand-dominated and was composed of a 0.5–12-cm-thick fine-to-very coarse sand with a mud cap in 0.5–3 cm thickness. Sections of the tsunami deposit with submillimeter and over 0.5-cm-thick sand layers overlying mud layers were found up to approximately 2.05 km inland (92.0 % of the inundation distance).

3.4.5 Run-up Height and Onshore Slope

Inundation heights and run-up heights (Fig. 3.3) generally range from 0 to 40 m above TP in coastal areas from Aomori Prefecture to northern part of Ibaraki Prefecture (Figs. 3.1b and 3.1c). Both of them showed the highest values in middle
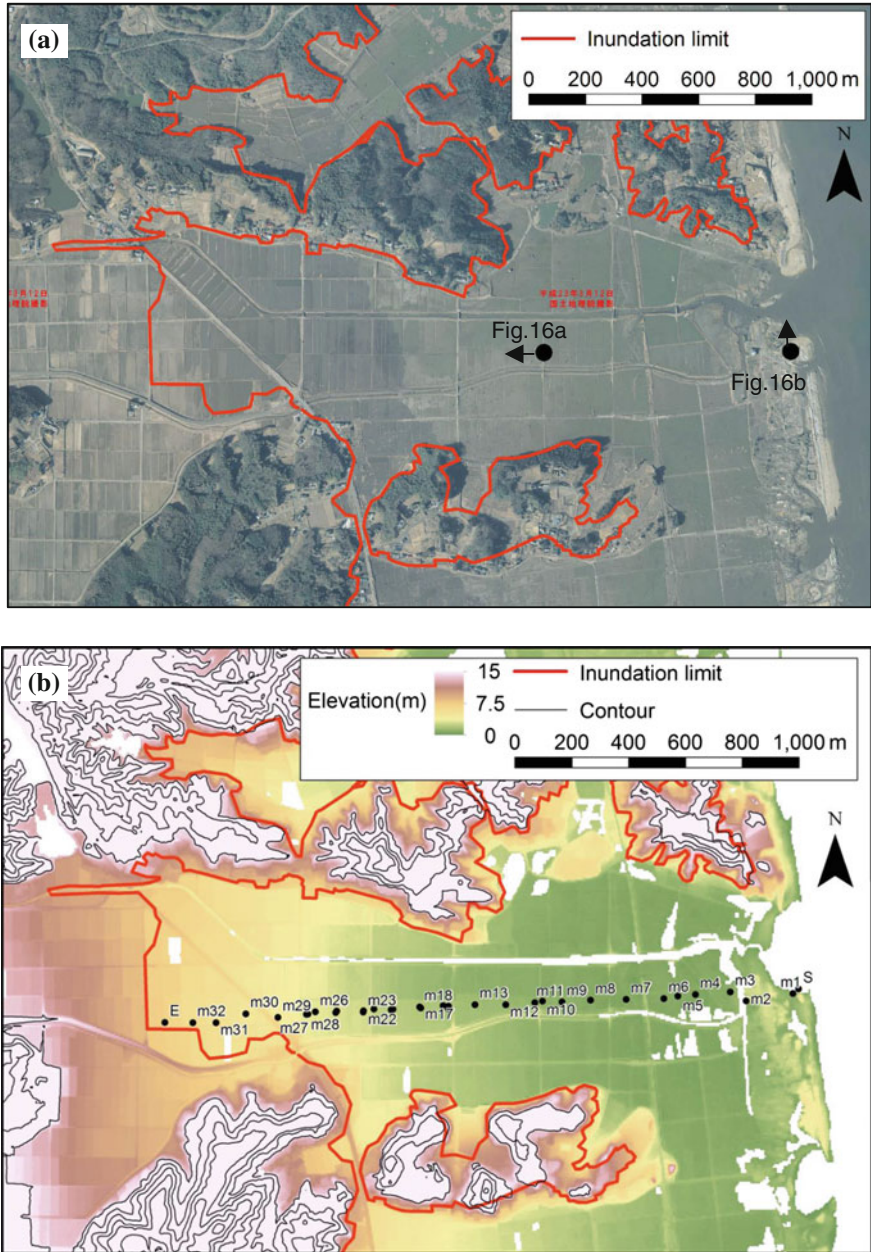
Fig. 3.15 **a** Aerial photograph (March, 2011) provided by GSI, inundation area, shooting location and direction of photograph in Fig. 3.16, **b** elevation map using 5 m mesh DEM, 5 m interval contour line (except for less than 10 m above TP), inundation area, and observation sites of the tsunami deposit in valley plain at Shinchi Town
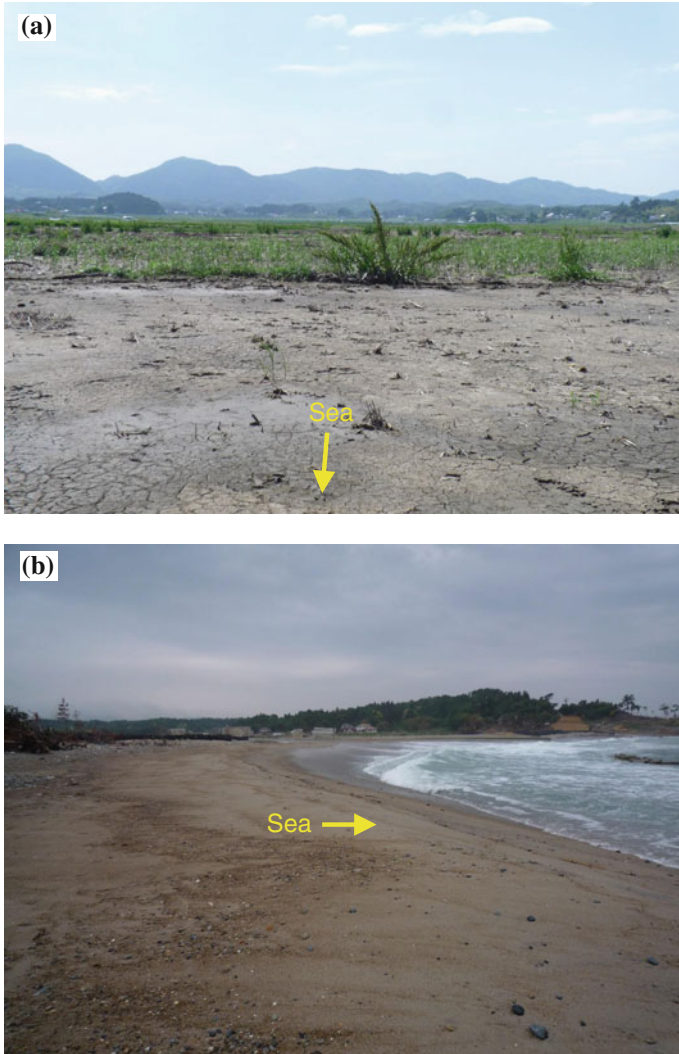
Fig. 3.16 Photographs of **a** erosion in sand beach and dune, **b** topography with steep longitudinal gradient in valley plain at Shinchi Town. Shooting locations and direction of photographs are shown in Fig. 3.15a

part of Sanriku Coast where indented coastlines characterized by rias are common. The values are mostly lower than 10 m above TP in Kamikita Plain and southern part of Iwaki Coast. Differences between inundation heights and run-up heights are not considerable at Kamikita Plain, Sanriku Coast, and Iwaki Coast. On the other hands, inundation heights are much higher than run-up heights in Sendai Plain.
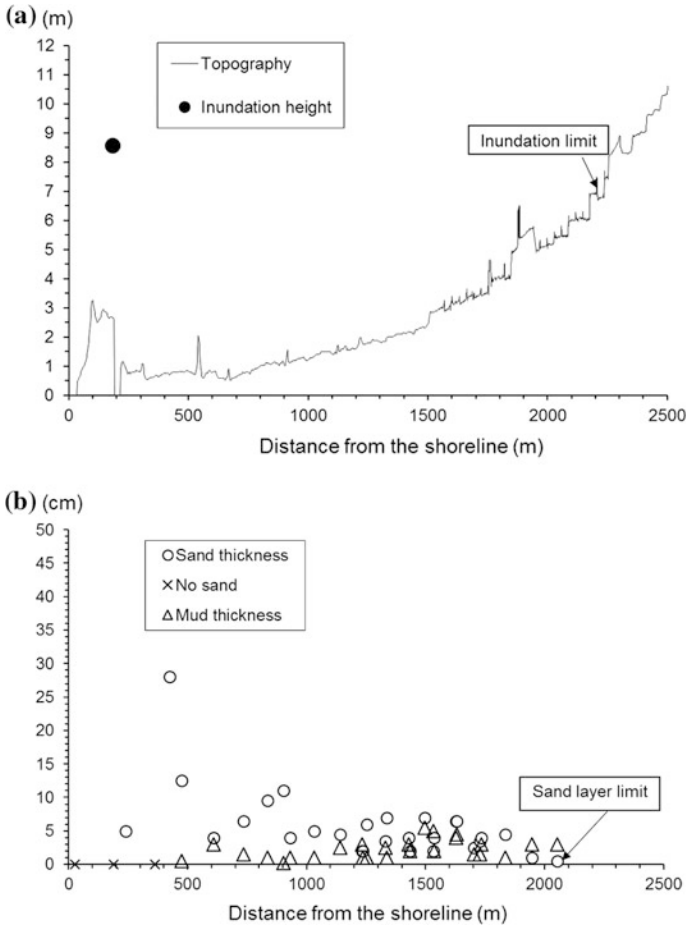
Fig. 3.17 a Elevation, inundation height above TP, and inundation limit, **b** sand and mud thickness in a valley plain at Shinchi Town

Maximum run-up height almost reached 40 m above TP (Fig. 3.19). The run-up height ranged from 6.8 to 39.4 m (TP) in RO type, from 5.7 to 30.1 m (TP) in RB type, and from 1.8 to 17.6 m (TP) in VO types (Table 3.1). The standard deviation of these coasts is large (3.6–7.8 m). In contrast, the heights are less than 3.3 m in VLO, SO, and SLO types. Furthermore, the standard deviation is also small (0.1–0.5 m).

Onshore slope from the shoreline to the tsunami run-up limit is less than 110 ‰. The slopes of RO, RB, and VO types are much larger than those of VLO, SO, and SLO types.

Fig. 3.18 28-cm-thick sand layer at 0.4 km from the shoreline (site m5 in Fig. 3.15b) in a valley plain at Shinchi Town
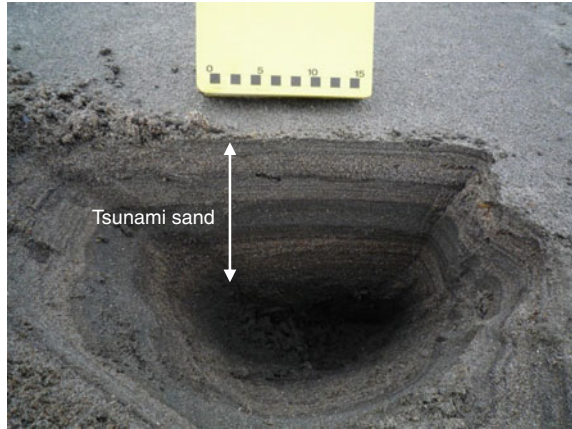

Fig. 3.19 Relationship between run-up height above TP and onshore slope from the coastline to inundation limit. Landforms are illustrated schematically in Fig. 3.2. The locations of the sampling points are shown in Fig. 3.4. Data are summarized in Table 3.1
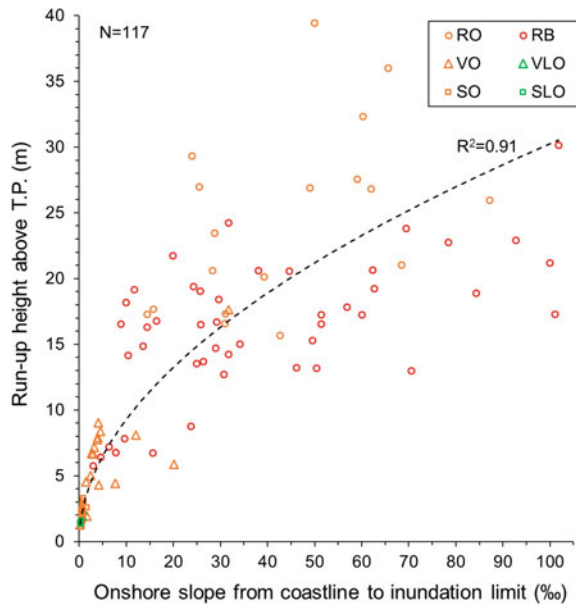
Run-up heights roughly increase with onshore slope (Fig. 3.19). The coefficient of correlation value (R^2) between them is 0.76 using power function. Both of the onshore slope and run-up heights in RO and RB types were much larger than those in VLO, SO, and SLO types. Onshore slope and run-up heights significantly varied in VO type. Differences of onshore slope and run-up heights between rias on open sea (RO) and rias facing bay (RB) were unclear.

Table 3.1 Run-up height and onshore slope in various types of coastal landforms

		RO	RB	VO	VLO	SO	SLO
Number of data		19	46	16	3	29	4
Run-up height (m)	Max	39.4	30.1	17.6	2.4	3.3	1.6
	Min	6.8	5.7	1.8	2.0	1.1	1.3
	Ave	23.6	16.2	6.7	2.2	2.1	1.4
	SD	7.8	5.2	3.6	0.2	0.5	0.1
Slope (‰)	Max	87.2	101.8	31.7	0.7	1.6	0.4
	Min	7.8	2.9	0.5	0.6	0.2	0.3
	Ave	41.6	38.9	6.7	0.7	0.6	0.3
	SD	21.4	28.1	8.3	0.1	0.3	0.1

3.5 Discussion

3.5.1 Tsunami Deposit

Tsunami sand widely deposited and reached hundreds of meters to a few kilometers inland in wide strand plain, narrow strand plain, and valley plain. Tsunami deposits were not clear, and erosional landforms due to backwash were common in a very minor, steep narrow valley plain along the ria coasts. However, Naruse et al. (2012) reported the formation of thick, sandy tsunami deposits at Rikuzentakata City where bay-head delta occurs at the head of rias (Fig. 3.1). A wave-dominated spit formed by the reworking of sediment supplied from the Kesen River extends along the coasts. Thus, beach sand was one of the major sources of the tsunami deposits.

Limited sand supply from beach and sand dune decreases sand deposition area (Nakamura et al. 2012). Grain size of beach and dune sand also controls the sand deposition area. Coastline is covered with fine- to medium-grained sand building beach and dune at the three transects, and sand erosion in beach and dune was observed.

The onshore tsunami deposit was mainly sourced from land (beach, sand dune, and paddy soil) around Sendai Plain. Numerical modeling of sediment transport on the Sendai Plain (Sugawara et al. 2014) suggested that bathymetry especially steep bathymetric profile of the shoreface limited erosion in seafloor. The slope in Sendai Bay is 1/50 to 1/100 from the shoreline to 5 m depth, 1/100 to 1/200 between 5 and 15 m depth, and less than 2/1000 deeper than 15 m depth (Udo et al. 2013). In contrast, Naruse et al. (2012) showed that tsunami deposits were transported from the seafloor of Hirota Bay or more pelagic region as well as beach in Rikuzentakata based on paleontological analysis and estimation of the total volume of the tsunami deposits. Offshore seafloor slope is almost constant, approximately 7/1000, from the shoreline to 80 m depth in Hirota Bay (Shimamura 2011). Furthermore, width of the bay mouth of Hirota Bay, ca. 6 km, characterized by ria coast is much narrower than that of Sendai Bay, ca. 77 km. The difference of bathymetry in these bays possibly influences the location of source area of the tsunami deposits.

We found landward-thinning trend of the sand thickness in wide strand plain and valley plain. Landward thinning of the sand is a typical feature for the tsunami deposit (Goff et al. 2012). It may relate to landward decrease in sediment supply and flow velocity and depth. However, this feature was not clear in narrow strand plain. It is possible that high flow velocity and depth and a large amount of sediment supply maintained near the inundation limit and run-up were forcibly stopped by high terraces in narrow strand plain. Distribution pattern of tsunami deposit was critically dependent on landform types.

Tsunami mud deposition in broad area is distinctive feature of the tsunami in Sendai coastal plain. Diatom assemblage showed that mud is originated from paddy soil in Sendai coastal plain (Szczuciński et al. 2012). As Sendai coastal plain is known for one of the largest cultivation area of rice, rice paddy field covered a considerable area of the lowland. Mud thickness slightly became thicker landward in wide strand plain and valley plain. It probably results from increase in rice paddy area eroded by tsunami with progression of inundation.

Sand thickness largely varied in a zone up to 1.0–1.5 km inland. The thickness of tsunami sand was likely to be sensitive to the local undulation of topography (Nishimura and Miyaji 1995). Yamada and Fujino (2013) pointed out that the thicknesses of the tsunami deposits near the shore were more variable than the deposits left inland, and it may have resulted from complex tsunami behavior due to the existence of protection forest and other artificial structures around the shore. Therefore, micro-topography may have affected thickness variation.

3.5.2 Run-up Height and Onshore Topography

Run-up heights varied significantly in this area (Figs. 3.1b and 3.19). Maximum wave heights offshore in 137–204 m depth from Sanriku Coast to northern Iwaki Coast were higher than those of Kamikita Plain and southern Iwaki Coast based on GPS buoys (Japan Meteorological Agency 2013; Kawai et al. 2013). Differences of the maximum wave heights were not clear between Sanriku Coast and northern Iwaki Coast. Therefore, variety of run-up heights observed at the study area (Fig. 3.19) might relate to the shape of local and regional onshore topography.

Our analysis showed that onshore slope from coastline to inundation limit was positively correlated with run-up height in general (Fig. 3.19). However, the relationship between run-up height and onshore slope was quite variable in RO, RB, and VO types rather than the other three types. For example, the run-up heights in valley plains with narrow valley floor and steep valley wall were higher than valley plains with wide valley floor and gentle valley wall. It is possible that the shape of valley also controls the run-up height in RO, RB, and VO types. On the other hand, run-up height is less than 3.3 m and a positive correlation between run-up height and onshore slope is unclear in SO, SLO, and VLO types, most of which face the Sendai Bay.

3.6   Conclusions

We showed the differences of distribution pattern of the tsunami deposit and run-up height in various types of coastal landform, such as rias, strand plain, and valley plain. Our main results were summarized below.

(1) Distribution pattern of tsunami deposit was critically dependent on landform types when large amount of sediment was supplied from the coasts.
(2) Balance between deposition and erosion might depend on onshore slope in coastal areas.
(3) Micro-topography may locally control thickness variation of the tsunami deposit.
(4) Run-up height generally relates to onshore slope from coastline to tsunami inundation limit, though morphology of the inundated lowlands such as valley floor and valley wall also influences run-up height.

It is necessary to consider the effect of seafloor bathymetry on run-up height in the future. In addition, relationship between onshore tsunami behavior and topography should be further discussed by combining field observation, numerical simulation, and flume experiment.

References

Abe T, Goto K, Sugawara D (2012) Relationship between the maximum extent of tsunami sand and the inundation limit of the 2011 Tohoku-oki tsunami on the Sendai Plain, Japan. Sed Geol 282:142–150

Chida N, Matsumoto H, Obara S (1984) Recent alluvial deposit and Holocene sea-level change on Rikuzentakata coastal plain, northeast Japan. Ann Tohoku Geogr Assoc 36(4):232–239 (in Japanese with English abstract)

Goff J, Chagué-Goff C, Nichol S, Jaffe B, Dominey-Howes D (2012) Progress in palaeotsunami research. Sed Geol 243–244:70–88

Goto K, Chagué-Goff C, Fujino S, Goff J, Jaffe B, Nishimura Y, Richmond B, Sugawara D, Szczuciński W, Tappin DR, Witter RC, Yulianto E (2011) New insights of tsunami hazard from the 2011 Tohoku-oki event. Mar Geol 290:46–50

Goto K, Sugawara D, Abe T, Haraguchi T, Fujino S (2012) Liquefaction as an important source of the A.D. 2011 Tohoku-oki tsunami deposits at Sendai Plain, Japan. Geology 40:887–890

Hayakawa YS, Oguchi T, Saito H, Kobayashi A, Baker RV, Pelletier DJ, McGuire L, Komatsu G, Goto K (2015) Geomorphic imprints of repeated tsunami waves in a coastal valley in northeastern Japan. Geomorphology 242:3–10

Ito A (1999) Holocene geomorphic development of the Kitakami River lowland, northeastern Japan. Kikan Chirigaku 51(1):1–18 (in Japanese with English abstract)

Jaffe BE, Gelfenbaum G (2002) Using tsunami deposits to improve assessment of tsunami risk. In: Solutions to coastal disasters '02, ASCE, pp 836–847

Kawaguchi K, Inomata T, Seki K, Fujiki T (2015) Annual report on nationwide ocean wave information network for ports and harbors (NOWPHAS 2013). Technical Note of the Port and Airport Research Institute, No. 1305

Kawai H, Satoh M, Kawaguchi K, Seki K (2013) Characteristics of the 2011 Tohoku tsunami waveform acquired around Japan by NOWPHAS equipment. Coast Eng J 55:1350008

Koike K, Tamura T, Chinzei K, Miyagi T (eds) (2005) Regional geomorphology of the Japanese Islands, vol. 3 geomorphology of Tohoku region. University of Tokyo Press, Tokyo

Komatsu G, Goto K, Baker VR, Oguchi T, Hayakawa YS, Saito H, Pelletier JD, McGuire L, Iijima Y, (2014) Effects of tsunami wave erosion on natural landscapes: examples from the 2011 Tohoku-oki Tsunami. In: Kontar Y, Santiago-Fandino V, Takahashi T (eds) Tsunami events and lessons learned: ecological and societal significance. Advances in natural and technological hazards research, vol 35. Springer, Berlin, pp 243–253

Koshimura S, Mofjeld HO, González FI, Moore AL (2002) Modeling the 1100 bp paleo tsunami in Puget Sound, Washington. Geophys Res Lett 29(20):1948

MacInnes BT, Bourgeois J, Pinegina TK, Kravchunovskaya EA (2009) Tsunami geomorphology: Erosion and deposition from the 15 November 2006 Kuril Island tsunami. Geology 37:995–998

Matsumoto H (1981a) Sea-level changes during the Holocene and geomorphic developments of the Sendai coastal plain, northeast Japan. Geogr Rev Japan 54(2):72–85 (in Japanese with English abstract)

Matsumoto H (1981b) Developmental process of alluvial plain related to the Holocene sea-level change. Sci Rep Tohoku Univ 7th Ser Geogr 31:151–171

Matsumoto H (1984) Beach ridge ranges on Holocene coastal plains in northeast Japan. Geogr Rev Japan, Ser A 57(10):720–738 (in Japanese with English abstract)

Miura O (1966) Coastal terraces and rias along the Kesennuma Bay, Miyagi Prefecture. Ann Tohoku Geogr Assoc 18(3):116–122 (in Japanese with English abstract)

Miura O (1968) Rias coast and coastal terraces of Sanriku, northeastern Japan. Geogr Rev Japan 41(12):732–747 (in Japanese with English abstract)

Miyauchi T (1987) Quaternary tectonic movements of the Kamikita Coastal Plain, Northeast Japan. Geogr Rev Japan, Ser. B 60(1):1–19

Miyauchi T (2001) Kamikita Plain. In: Koike K, Machida H (eds) Atlas of Quaternary marine terraces in the Japanese Islands. University of Tokyo Press, Tokyo, pp 27–29 (in Japanese)

Nakamura Y, Nishimura Y, Putra PS (2012) Local variation of inundation, sedimentary characteristics, and mineral assemblages of the 2011 Tohoku-oki tsunami on the Misawa coast, Aomori, Japan. Sed Geol 282:216–227

Nanayama F, Satake K, Furukawa R, Shimokawa K, Atwater BF, Shigeno K, Yamaki S (2003) Unusually large earthquakes inferred from tsunami deposits along the Kuril trench. Nature 424:660–663

Naruse H, Arai K, Matsumoto D, Takahashi H, Yamashita S, Tanaka G, Murayama M (2012) Sedimentary features observed in the tsunami deposits at Rikuzentakata City. Sed Geol 282:199–215

National Astronomical Observatory of Japan (ed) (2013) Chronological scientific tables 2014. Maruzen, Tokyo

Nishimura Y, Miyaji N (1995) Tsunami deposits from the 1993 Southwest Hokkaido earthquake and the 1640 Hokkaido Komagatake eruption, northern Japan. Pure and Applied Geophysics 144:719–733

Richmond BM, Szczuciński W, Chagué-Goff C, Goto K, Sugawara D, Witter R, Tappin DR, Jaffe BE, Fujino S, Nishimura Y, Goff J (2012) Erosion, deposition and landscape change on the Sendai coastal plain, Japan, resulting from the March 11, 2011 Tohoku-oki tsunami. Sed Geol 282:27–39

Shimamura K (2011) The relationship between the topographic features of bay and the tsunami-height-topographic study on the tsunami-height in the 2011 off the Pacific coast of

Tohoku earthquake of bay and the tsunami-height. Bull School Ind Eng Tokai Univ 4:1–8 (in Japanese with English abstract)

Shishikura M, Fujiwara O, Sawai Y, Namegaya Y, Tanigawa K (2012) Inland-limit of the tsunami deposit associated with the 2011 off-Tohoku earthquake in the Sendai and Ishinomaki Plains, Northeastern Japan. Ann Rep Active Fault Paleo Earthq Res 12:45–61 (in Japanese with English abstract)

Sugawara D, Takahashi T, Imamura F (2014) Sediment transport due to the 2011 Tohoku-oki tsunami at Sendai: results from numerical modeling. Mar Geol 358:18–37

Suzuki T (1989) Late Quaternary crustal movements deduced from marine terraces and active faults, Joban coastal region, northeast Japan. Geogr Rep Tokyo Metrop Univ 24:31–42

Szczuciński W, Kokociński M, Rzeszewski M, Chagué-Goff C, Cachão M, Goto K, Sugawara D (2012) Sediment sources and sedimentation processes of 2011 Tohoku-oki tsunami deposits on the Sendai plain, Japan-Insights from diatoms, nannoliths and grain size distribution. Sed Geol 282:40–56

Takashimizu Y, Urabe A, Suzuki K, Sato Y (2012) Deposition by the 2011 Tohoku-oki tsunami on coastal lowland controlled by beach ridges near Sendai, Japan. Sed Geol 282:124–141

Tamura T, Masuda F (2005) Bed thickness characteristics of inner-shelf storm deposits associated with a transgressive to regressive Holocene wave-dominated shelf, Sendai coastal plain, Japan. Sedimentology 52:1375–1395

The 2011 Tohoku Earthquake Tsunami Joint Survey Group (2011) The 2011 off the Pacific coast of Tohoku earthquake tsunami information. http://www.coastal.jp/ttjt/

The Japan Meteorological Agency (2013) The report on the 2011 off the Pacific coast of Tohoku Earthquake. Technical report of the Japan Meteorological Agency 133

Udo K, Tanaka H, Mano A, Takeda Y (2013) Beach morphology change of southern Sendai coast due to 2011 Tohoku earthquake Tsunami. J JSCE, Ser B2 (Coastal Engineering) 69:1391–1395 (in Japanese with English abstract)

Yagi H, Suzuki T (2001) Sanriku-nanbu to Joban. In: Koike K, Machida H (eds) Atlas of Quaternary marine terraces in the Japanese Islands. University of Tokyo Press, Tokyo, pp 29–32 (in Japanese)

Yamada M, Fujino S (2013) Sedimentary characteristics of the onshore tsunami deposits formed by the 2011 Tohoku-oki tsunami in coastal lowlands, Ibaraki and Chiba prefectures. J Sedimentol Soc Japan 72(1):13–25 (in Japanese with English abstract)

Yonekura N (1966) Geomorphic development of northern Rikuchu coastal region, north-eastern Japan. Geogr Rev Japan 39(5):311–323 (in Japanese with English abstract)

Yoshikawa T (1964) On the geomorphic development of Ria coasts in the Japanese Islands. Quat Res (Daiyonki-kenkyu) 3:290–296 (in Japanese with English abstract)

Yoshikawa T (1997) Continental shelf. Kokon Shoin, Tokyo (in Japanese)